

# Soldering of Nanotubes onto Microelectrodes

Dorte Nørgaard Madsen,<sup>†</sup> Kristian Mølhave,<sup>†</sup> Ramona Mateiu,<sup>†</sup>  
Anne Marie Rasmussen,<sup>‡</sup> Michael Brorson,<sup>‡</sup> Claus J. H. Jacobsen,<sup>‡</sup> and  
Peter Bøggild<sup>\*,†</sup>

Mikroelektronik Centret, Technical University of Denmark,  
DK-2800 Kgs. Lyngby, Denmark, and Haldor Topsøe A/S,  
Nymøllevej 55, DK-2800 Lyngby, Denmark

Received September 17, 2002; Revised Manuscript Received November 6, 2002

## ABSTRACT

Suspended bridges of individual multiwalled carbon nanotubes were fabricated inside a scanning electron microscope by soldering the nanotube onto microelectrodes with highly conducting gold–carbon material. By the decomposition of organometallic vapor with the electron beam, metal-containing solder bonds were formed at the intersection of the nanotube and the electrodes. Current–voltage curves indicated metallic conduction of the nanotubes, with resistances in the range of 9–29 k $\Omega$ . Bridges made entirely of the soldering material exhibited resistances on the order of 100  $\Omega$ , and the solder bonds were consistently found to be mechanically stronger than the carbon nanotubes.

Carbon nanotubes have been proposed as prototypical nanoscale building blocks because of their unique mechanical and electrical properties.<sup>1</sup> To explore their potential in physics, chemistry, and biology, a number of methods have been employed to form electrical and mechanical connections to devices and nanostructures.<sup>2–5</sup> We present an in situ method for the highly conductive attachment of nanoscale components by the use of a gold–carbon composite soldering material deposited by a focused electron beam. This method does not require electrical contact to the electrodes or the component and allows for the assembly of 3D structures.

We used a Philips XL30 ESEM-FEG environmental scanning electron microscope, operating at a water vapor pressure of 100 Pa. Dimethylacetylacetonate gold(III), which has a vapor pressure of 1 Pa at 25 °C, was placed in a container with a narrow bore tube to control the diffusion of organometallic vapor onto the sample. The electron beam locally decomposes the organometallic compound and thereby deposits a material with metallic content.<sup>6</sup> Using a 2-mm-long tube with a diameter of 0.8 mm, we obtained a growth rate of 500 nm/min. Tips with lengths of more than 10  $\mu\text{m}$  could be grown without a significant decrease in the growth rate. All depositions were made at room temperature. A nanomanipulator stage inside the chamber was used to move a silicon chip with two cantilever microelectrodes.<sup>7</sup> The electrodes were connected to a DC voltage source, and the current was monitored continuously (see Figure 1a). Samples

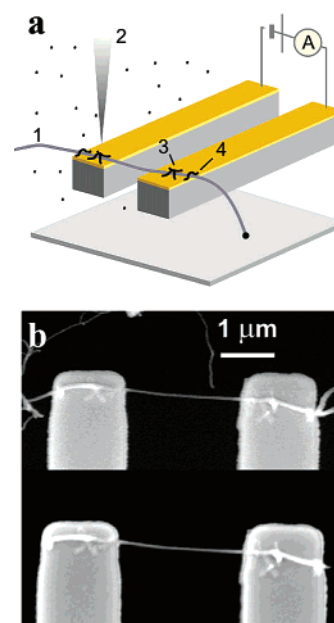


**Figure 1.** (a) Illustration of two microelectrodes positioned close to a multiwalled nanotube (1) extending from a catalyst particle on a substrate. Organometallic molecules decomposed by the electron beam (2) are deposited to form a cross-shaped solder bond (3) and a protective bond (4) near the edge of the electrode. (b) ESEM image of a carbon nanotube across two electrodes, connected by soldering bonds and protective bonds (top). When the electrode pair is withdrawn, the nanotube breaks at the protective bonds (bottom).

\* Corresponding author. E-mail: pb@mic.dtu.dk.

<sup>†</sup> Technical University of Denmark.

<sup>‡</sup> Haldor Topsøe A/S.

of free-standing multiwalled carbon nanotubes (MWNTs) were prepared<sup>8</sup> and characterized by transmission electron

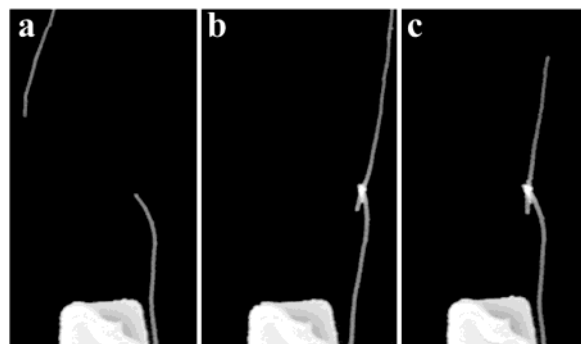


**Figure 2.** SEM image sequence of tube-to-tube soldering showing the approach of a nanotube soldered to a microelectrode toward a MWNT extending from the substrate (a) and subsequent soldering of the tube ends (b). Withdrawal of the electrode broke the nanotube and not the bond (c).

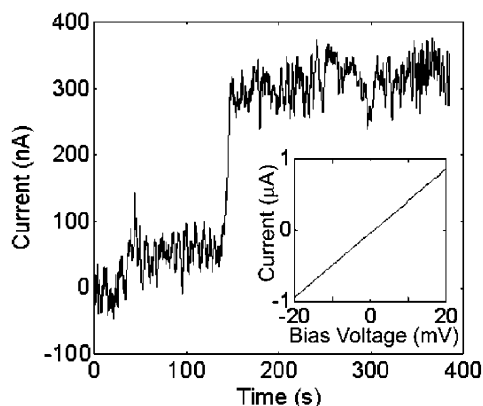


**Figure 3.** Current vs time during soldering of the MWNT using the electron beam. A fixed voltage of 10 mV is applied across the microelectrodes. During the formation of the second soldering bond, the current suddenly increased to a stable 300 nA. The IV characteristic (inset) was found to be linear.

microscopy (TEM), which revealed the presence of more than 20- $\mu\text{m}$ -long, 80–120-nm-wide MWNTs. In the ESEM, a microelectrode pair was aligned to a nanotube extending from the sample so that both electrodes touched the nanotube. By slowly scanning the beam across the nanotube at the point of contact to the first electrode, two cross-shaped gold–carbon soldering bonds were formed.

The deposition of a set of protective bonds near the edge of the microelectrodes allowed us mechanically to break off the MWNT parts extending beyond the electrodes without damaging the soldering bonds (see Figure 1b, lower panel). We consistently observed the MWNTs to break rather than the protective bonds, both for tube–electrode bonds (Figure 1) and for tube–tube bonds, as shown in Figure 2. To avoid unwanted contamination of the nanotubes by soldering material, we avoided imaging the suspended part of the nanotubes at high magnification.

For all of the examined bridges, electrical contact was established during the soldering procedure at the second electrode. In the example shown in Figure 3, the current increased in two steps, first from 0 to 60 nA and then abruptly to 300 nA, at a bias voltage of 10 mV. A linear current–voltage curve was measured, indicating metallic

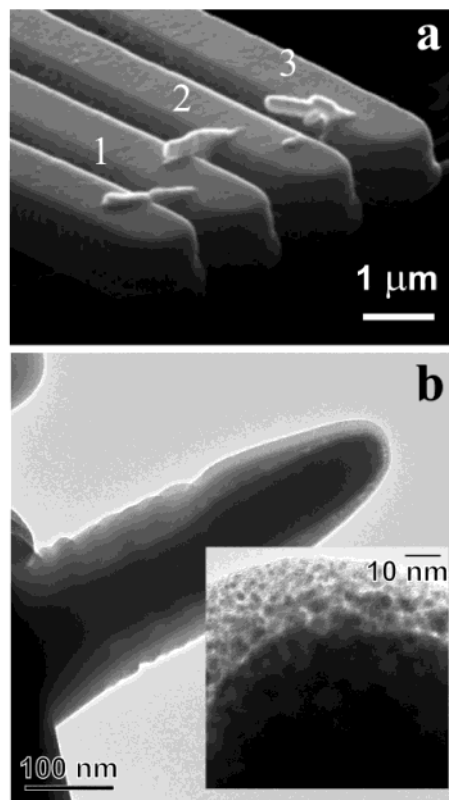


**Figure 4.** (a) SEM image of three bridges of soldering material deposited between microelectrodes by scanning the electron beam across the gaps at different speeds (fastest for bridge 1). The resistances were 127  $\Omega$  for bridge 1 and 520  $\Omega$  for bridge 2. Bridge 3 did not connect to both electrodes. (b) TEM image of a beam of soldering material, showing a dense core encapsulated in a porous crust. In the inset, the porous crust structure with 3–5-nm nanoparticles can be seen.

conduction (Figure 3, inset), and the resistance was 27 k $\Omega$ . We connected four nanotubes and every time obtained reliable ohmic contacts upon soldering to the second electrode, with resistances of 9, 11, 27, and 29 k $\Omega$ , with no clear correlation to the length of the MWNT bridge. The resistances of the nanotube bridges were unaffected by the breaking of the nanotube extensions and by the deposition of the protective bonds and were found to be constant in air for days.

We verified that the soldering material itself was conducting by depositing gold–carbon bridges between microelectrode pairs (Figure 4a) and measuring the IV characteristics. All of the bridges that connected properly to both microelectrodes, such as bridges 1 and 2 in Figure 4a, showed ohmic resistances between 80 and 520  $\Omega$ . By estimating the cross section of the bridges from SEM images and taking a serial resistance of roughly 60  $\Omega$  into account, we obtained resistivities down to  $10^{-4}$   $\Omega$  cm. TEM analysis of the soldering material revealed a gold–carbon composite structure with a porous crust of 3–5-nm nanoparticles around a dense core (Figure 4).

We also attached MWNTs to microelectrodes by means of nonmetallic carbonaceous material; these devices showed electrical conduction in the megaohm range. This strongly

indicates that the metal content of the soldering material is necessary for good electrical contact.

The question regarding the contribution of individual shells in MWNTs to the conductivity of the tube is still not resolved. Frank et al.<sup>9</sup> observed a consistent resistance of 13 k $\Omega$  for nearly defect-free arc-discharge-grown MWNTs, whereas Collins and co-workers<sup>10</sup> found lower values (5–15 k $\Omega$ ) and evidence of several contributing shells at low bias. Chemical-vapor-deposited nanotubes generally contain more structural defects than arc-discharge-grown nanotubes, which leads to a curving of the nanotubes (see Figure 1). The reason for the relatively small resistances (compared to those in ref 9 and 10) observed in our CVD-grown nanotubes is not clear. It has been proposed that structural defects may decrease the intershell resistivity. In our case, this could lead to more shells contributing to the transport, thus partially compensating for the reduced resistance of each shell.

The resistivity of the soldering material is slightly larger than the value of  $1.3 \times 10^{-5} \Omega \text{ cm}$  reported by Bietsch et al. for microcontact-printed pure-gold nanowires of similar dimensions<sup>11</sup> and 2 orders of magnitude larger than that of bulk gold. For electron-beam-deposited nanowires, resistances as small as ours have been obtained by heating the sample to 80 °C during deposition to increase the relative content of gold.<sup>6</sup> These values were obtained only after annealing at 180 °C, which further reduced the resistivity by 2–3 orders of magnitude. One possible explanation for the high conductivity of our material achieved at room temperature without annealing could be that the presence of H<sub>2</sub>O in the sample chamber reduces the relative amount of carbon, as suggested by Folch and co-workers.<sup>12</sup> This could be clarified by analyzing the chemical composition of the soldering material deposited at different vapor pressures.

The method of nanosoldering presented here does not

depend on the particular nanocomponent or on the electrodes. It involves no lithographic steps or electrical connections such as in spot welding,<sup>5</sup> and it is straightforward to achieve accurate alignment. The soldering bonds were found to be mechanically strong compared to the MWNTs. To investigate this quantitatively, a piezo-resistive force sensor will be integrated in the setup. We anticipate automated electron-beam nanosoldering to be useful for quickly connecting complex circuitry consisting of nanoscale components in a way similar to the soldering of electronic components on the macroscale.

**Acknowledgment.** We acknowledge financial support from the Danish Technical Research Council (NANOHAND talent project).

## References

- (1) Collins, P. G.; Avouris, P. *Sci. Am.* **2000**, 283, 38.
- (2) Williams, P. A.; Papadakis, S. J.; Falvo, M. R.; Patel, A. M.; Sinclair, M.; Seeger, A.; Helser, A.; Taylor, R. M.; Washburn, S.; Superfine, R. *Appl. Phys. Lett.* **2002**, 80, 2574.
- (3) Yu, M. F.; Dyer, M. J.; Skidmore, G. D.; Rohrs, H. W.; Lu, X. K.; Ausman, K. D.; Von Ehr, J. R.; Ruoff, R. S. *Nanotechnology* **1999**, 10, 244.
- (4) Banhart, F. *Nano Lett.* **2001**, 1, 329.
- (5) Cumings, J.; Zettl, A. *Science (Washington, D.C.)* **2000**, 289, 602.
- (6) Kooops, H. W. P.; Schossler, C.; Kaya, A.; Weber, M. *J. Vac. Sci. Technol., B* **1996**, 14, 4105.
- (7) Bøggild, P.; Hansen, T. M.; Tanasa, C.; Grey, F. *Nanotechnology* **2001**, 12, 331.
- (8) Wang, X. B.; Liu, Y. Q.; Zhu, D. B. *Chem. Commun.* **2001**, 751.
- (9) Franks, S.; Poncharal, P.; Wang, Z. L.; Heer, W. A. *Science (Washington, D.C.)* **1998**, 280, 1744.
- (10) Collins, P. G.; Avouris, P. *Appl. Phys. A* **2002**, 74, 329.
- (11) Bietsch, A.; Michel, B. *Appl. Phys. Lett.* **2002**, 80, 3346.
- (12) Folch, A.; Tejada, J.; Peter, C. H.; Wrighton, M. S. *Appl. Phys. Lett.* **1995**, 66, 2080.

NL0257972